GALLIUM INDIUM ARSENIDE PHOTODIODES

K. AHMAD and A. W. MABBITT

Plessey Research (Caswell) Ltd., Allen Clark Research Centre, Caswell, Towcester, Northants., England

(Received 5 June 1978; in revised form 2 October 1978)

Abstract—Efficient PIN photodetectors optimised for use at $1.15 \,\mu$ m have been developed employing expitaxially grown $Ga_{0.7}In_{0.3}As$ layers on GaAs substrates, with graded composition buffer regions to minimise lattice mismatch. Device geometries can be readily tailored for fibre optic or ranging applications, although the large area photodiodes described here were intended for relatively low frequency ranging systems. Dark currents less than $0.1 \,\mu$ A at 9 volts reverse bias and quantum efficiencies in excess of 80% at $1.15 \,\mu$ m were achieved by employing a simple mesa structure with SiO_2 passivation. In forward bias a diode ideality factor of n=1.8 was typical corresponding to mixed diffusion and recombination currents. Although the reverse characteristics show leakage dominated currents, the dark current is substantially lower than that of commercially available Ge photodiodes intended for similar applications. Measured rise and fall times of 10 nSec were essentially RC limited into 50 ohm loads, and it is expected that faster devices for fibre optic applications would result by appropriate reduction of device area and background doping level.

1. INTRODUCTION

The advantages to be gained in operating fibre optic communication systems in the wavelength range 1-1.3 μ m have led to widespread interest in the development of suitable sources and detectors optimised for use at longer working wavelengths [1]. In particular, the possibility of varying the optical band-gap with alloy composition [2, 3] afforded by certain ternary III-V alloys such as $Ga_{1-x}In_xAs$ together with the advantages of expitiaxial growth techniques makes such materials attractive for the fabrication of photodetectors and LEDs. We describe here the development of $Ga_{0.70}In_{0.30}As$ photodetectors optimised for use at 1.15 μ m with device geometries which can be readily tailored for fibre optic or rangefinding applications.

Epitaxially grown Ga_{1-x}In_xAs was chosen as a logical extension to an earlier programme which led successfully to the development of a 1.06 μ m LED released to Defence Standard specifications [4-6]. Devices were initially fabricated with grown-in p-n junctions as our previous LED experience had shown that best performance was obtained with such junctions compared to diffused junction diodes in Ga_{1-x}In_xAs and Ga_{1-x}In_xP. However, diffused junction GaAs LEDs exhibited harder reverse breakdown characteristics than grown-in junctions so that diffused junctions in Ga1-x Inx As were also investigated with a view to obtaining lower dark currents. An estimate of the order of magnitude of reverse currents attainable with n-type epilayers of Ga1-x Inx As could be obtained by forming Au/Ti Schottky barriers. Such devices showed reverse saturation currents in the range 20-50 nA for 1 mm² active areas, although as a result of light absorbtion in the metal overlayer the quantum efficiency is necessarily low.

2. GROWTH OF EPITAXIAL Gal-xInxAs

The photodetectors were fabricated from epitaxially grown Ga_{1-x}In_xAs ternary alloys prepared by vapour

phase epitaxy (VPE) on commercially available low defect GaAs substrates. The hydride VPE growth technique employed[4] allows precise control of material parameters together with flexibility regarding layer configurations and thicknesses. The (100) oriented GaAs substrates are etched to eliminate sub-surface work damage before placing in a quartz reactor tube surrounded by a three zone resistance heated furnace with accurately controlled temperature zones. The experimental arrangement is shown schematically in Fig. 1. The gallium and indium sources have separately metered HCl gas supplies for use as a transporting agent. Typically this pickup zone is maintained at 850°C, at which Ga and In are transported as their volatile monochlorides. The metal monochlorides are carried in a palladium diffused hydrogen ambient into a mixing zone at 875°C where they are mixed with a metered flow of 5% AsH₃/H₂. The HCl flow rates controlling the alloy composition are monitored using electronic mass flow controllers resul-

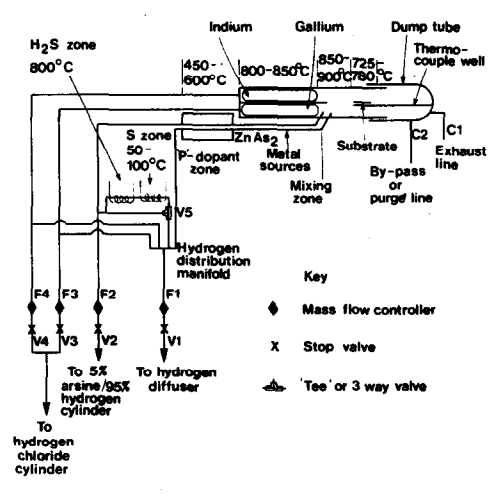


Fig. 1. Schematic of VPE growth reactor

ting in a run-to-run composition reproducibility of $\pm 0.1\%$ for alloy compositions up to 30% In. In addition facilities are provided to vary the HCl flow rates so that it is possible to obtain continuously graded layers, enabling the growth of a graded composition buffer layer between the substrate and the constant composition layer in which the device is fabricated [3].

The doping levels in the epilayer can be adjusted by introducing gas phase dopants into the mixing zone. The n-type dopant is sulphur derived from a H_2S flow and the p-type dopant is Zn from a $ZnAs_2$ source. The dopant sources can be switched during a growth run allowing the preparation of grown-in junctions. The minimum controllable n-type doping levels attained were of the order of $1-2\times10^{16}$ electrons/cm³ while the p-type doping level was adjusted in the region 5×10^{17} holes/cm³. The n-layer doping density was inferred from mercury-probe Schottky barrier capacitance measurements carried out on test n-type epilayers, whereas the hole concentration in the thin p-type layers could be estimated from Hall measurements. A typical epilayer grown for detector fabrication consisted of:

GaAs (100) Si doped substrate + n-type Ga_{1-x}In_xAs graded composition layer with a grading rate of approx. 1% In per micron

- + n-type $Ga_{0.70}In_{0.30}As$ constant composition layer about $5 \mu m$ thick with doping density $\sim 2 \times 10^{16}$ electrons/cm³
- + p-type $Ga_{0.70}In_{0.30}As$ constant composition layer 1-3 μ m thick with doping density $\sim 1 \times 10^{18}$ holes/cm³.

3. MATERIAL ASSESSMENT

Compositional reproducibility was ascertained by Xray measurement of the lattice parameter and interpolation according to Vegards rule [7], confirming that a run-to-run consistancy of $\pm 0.1\%$ In could be established under optimum growth conditions. In addition, the half widths of the X-ray lines give a qualitative indication of spatial compositional uniformity of the epilayer, which was of high order after appropriate calibration of flow rates. Device quality epilayers showed mirror finish surfaces with the faint "cross-hatched" appearance characteristic of epitaxial growth with lattice mismatch relative to the substrate. The relative magnitude of the crosshatching appeared to show no reproducible correlation with any subsequent device characteristic. The "crosshatched" surfaces observed in certain III-V alloy epitaxial systems are believed to reflect slip processes involving the misfit dislocations formed as a result of inherent lattice mismatch[8, 9], although detailed mechanisms are not entirely clear.

Transmission electron microscopy (TEM) of thinned layers confirmed that a relatively high defect density was present, with the lattice mismatch partially taken up by strain and partially by formation of misfit dislocation arrays. The dislocation density was estimated to be in the region 10⁶-10⁷ cm³, with considerable variation from layer to layer. For some epilayers large concentrations of stacking fault clusters were observed. These are believed to arise from substrate surface imperfections and/or contamination and may be minimised by adequate pre-

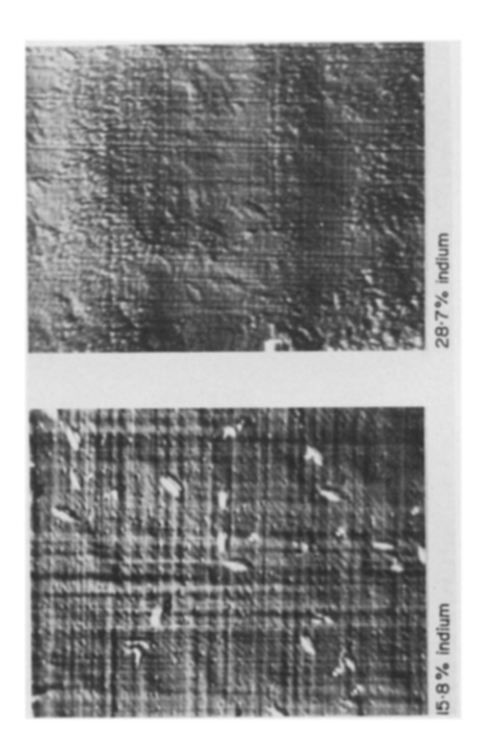
paration of the substrate surface prior to growth. The dislocation density depended markedly on the growth conditions, as expected, and particularly on the grading rate, with an optimum grading rate in the region of 1% In per micron. However, no obvious correlation of observed defect densities with subsequent device characteristics could be established. An alternative method often employed to minimise the effects of lattice mismatch in III-V ternary alloys is to step-grade in the buffer layer[2, 3, 10]. A number of epilayers grown with step-graded buffer layers were assessed, although devices fabricated from such layers were found to show similar overall performance to those employing linearly-graded buffer layers.

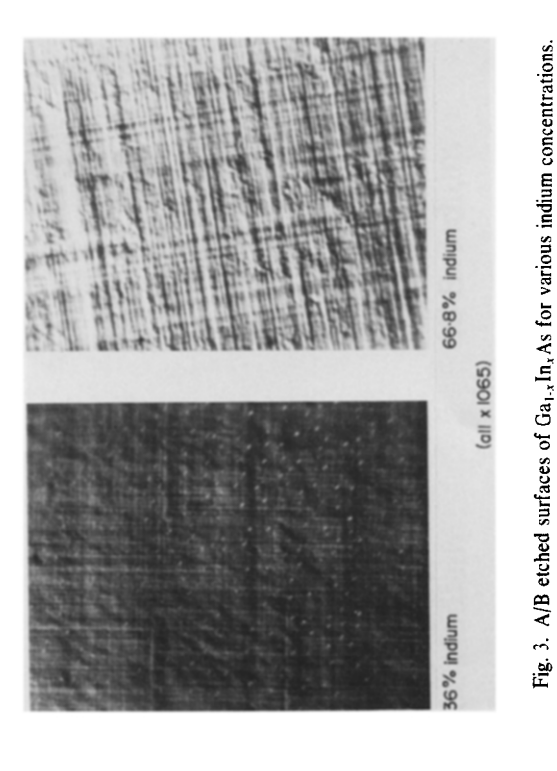
It has been suggested [3, 10] that abrupt composition steps in the buffer layer may effectively "bend over" inclined misfit dislocations and consequently reduce the number of defects emerging ultimately into the constant composition layer. This was verified for some of the step-graded layers by cleaving and etching in A/B etchant[11, 12]. Figure 2 shows a step graded layer (a) before and (b) after A/B etching, viewed in Nomarski interference contrast mode. It is clear that relatively fewer etch pits are seen in the constant composition top layer than in the step graded buffer layer. However, preliminary TEM examination of the defect structures in both step-graded (with constant 2% Indium steps) and linearly graded layers grown under otherwise similar conditions have yielded comparable dislocation densities so that step grading may not necessarily be preferable.

In order to assess the feasibility of extending the peak photo response of the diodes to around 2.1 μ m, a preliminary study of epilayer quality was undertaken by progressively increasing the indium concentration in the constant composition region in the range 15-65% In. Step-wise A/B etching of epilayers containing 16, 24, 30 and 55% Indium and inspection of the resulting etch pit density (EPD) patterns in interference contrast mode showed that although high defect densities were present in the epilayers as expected from the inherent large lattice mismatches, no well-defined composition dependance of the EPD patterns or trend could be discerned in the range studied. Differences in the growth conditions of the epilayers were found to lead to more variable EPD topologies than compositional variations. Typical patterns obtained after 1 min A/B etching are reproduced in Fig. 3 for various compositions of Indium. EPD counts after shallow A/B etching revealed that dislocations emerging at angles to the surface were in the range $1-6 \times 10^7$ cm⁻² with considerable variation from layer to layer. Progressive A/B etching into the graded composition layer led to EPD topologies that were difficult to interpret unambiguously.

4. DEVICE FABRICATION

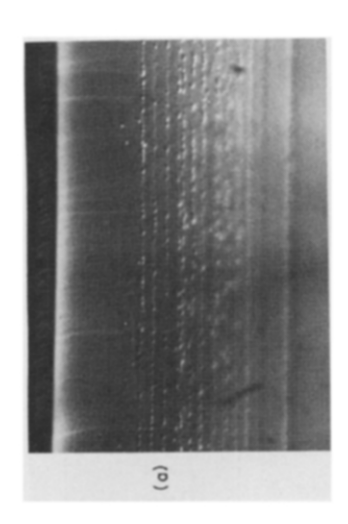
Photodetectors were constructed incorporating either diffused or grown-in p^+n junctions using conventional photolithography and metallization techniques. Diffused junctions were obtained by shallow Zn diffusions in an evacuated, sealed quartz ampoule using either 5% Zn/Ga or ZnAs₂ sources. Loss of arsenic from the surface of





(P)

Fig. 2. (a) Before A/B etching. Cleaved section through layer. Normarski interference contrast. (b) After 1 mm A/B etch. Normarski interference contrast.



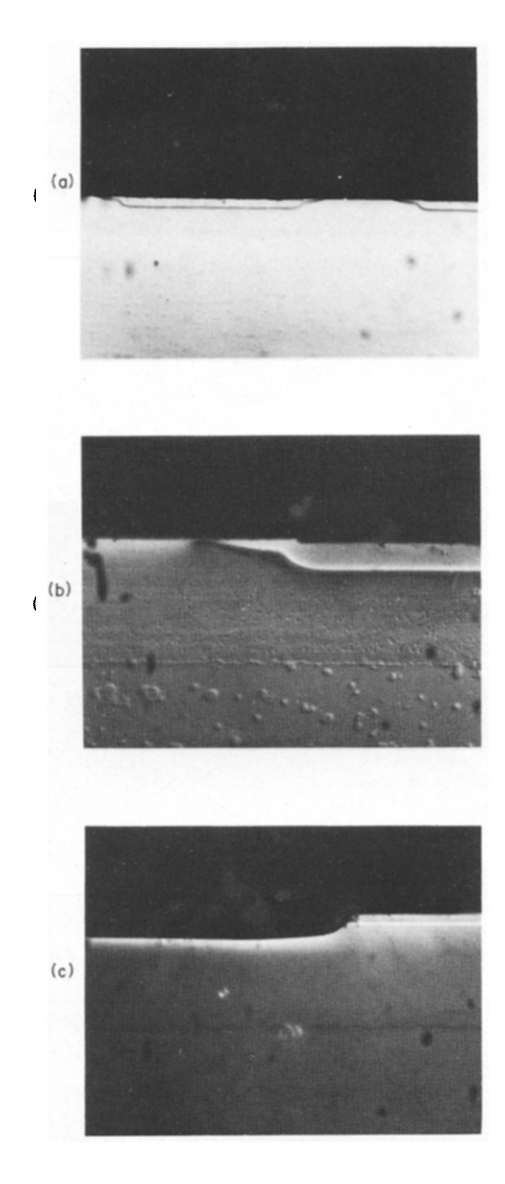


Fig. 4. (a) Section through epilayer after Zn diffusion, (b) Detail of diffusion "winging" effect, (c) Shallow-mesa device structure.

the epilayers was minimised during diffusion by including a substantial amount of GaAs ballast material in the ampoule, thereby maintaining an arsenic overpressure. Test diffusions in the range 700-900°C showed that diffusion of Zn was much more rapid in the $Ga_{1-x}In_xAs$ alloy than in GaAs, with poor reproducibility and uneven diffusion fronts at temperatures above 800°C. The relatively rapid diffusion of Zn into $Ga_{1-x}In_xAs$ is thought to be due to the high defect density in the epilayer. However, reproducible diffusion fronts in the range 2-3 μ m could be obtained using a ZnAs₂ source at 650°C.

Localization of the Zn diffusion was obtained by photolithographic definition of holes in a predeposited $0.3 \,\mu\text{m}$ silox layer. Devices fabricated in this way showed surprisingly high and variable reverse leakage currents in the range $2-20\,\mu\text{A}$ at $10\,\text{V}$ bias. Cleaving and staining showed that substantial "winging" of the diffusion front occurs with a deposited silox diffusion mask leading to poor localization of the active area, as shown in Fig. 4, and hence relatively high excess surface leakage currents. The "winging" effect observed is thought to be caused by Zn penetration along the silox/GaInAs interface. A substantial reduction in the reverse $(0.1\,\mu\text{A} \otimes 10\,\text{volts})$ current could be obtained by removing the diffusion winging with a shallow mesa etch. The resulting section through a device edge is shown in Fig. 4(c).

As a result of the poor masking afforded by the SiO₂ to Zn diffusion in the GalnAs layer no major advantage was to be gained in adopting a diffused junction approach. Consequently grown-in junction shallow mesa devices with junction depths in the region 2-3 μ m were fabricated and assessed for reverse current and quantum efficiency at 1.15 μ m. The photodiodes have an active area of 1 mm² with SiO₂ antireflection coating and Ti/Au p-face ring contact metallization. The overall slice thickness is ~100 μ m with a sintered Au/Ge/In metallization on the n^+ GaAs substrate.

5. DEVICE CHARACTERISTICS

A typical reverse current characteristic of a Ga_{0.70}In_{0.30}As photodetector is reproduced in Fig. 5,

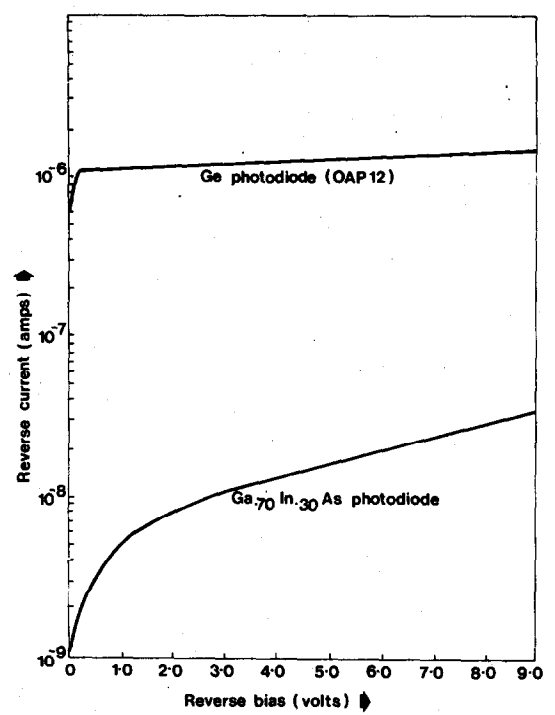


Fig. 5. Typical reverse characteristics of GaInAs photodiode compared with Ge photodiode.

together with that of a commercially available Ge photodiode. Dark currents less than $0.1\,\mu\text{A}$ at 10 volts bias could readily be obtained using good quality epilayers, although some variability in the reverse characteristics was noted for different layers. The reverse current characteristic exhibits a substantial excess leakage component since extrapolation of the forward current characteristic to intersect the current axis implied an "ideal diode" reverse saturation current of between 1 and 3 nA. It is expected that this excess current is predominantly surface leakage, although excess bulk leakage as a result of high defect densities may be significant [13]. The forward current characteristics of the diodes yielded a "diode ideality factor" n = 1.8, implying a significant recombination component.

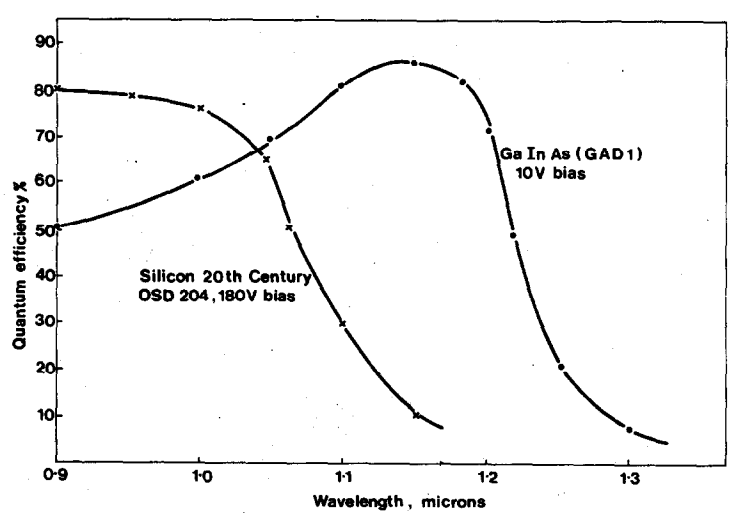


Fig. 6. Typical spectral response of GaInAs photodiode compared to Si PIN device.

Measurements of device quantum efficiency were carried out using a calibrated pyroelectric ceramic detector as standard. For devices constructed in high quality epilayer quantum efficiencies at 1.15 µm in excess of 80% were obtained with best values being 89% at zero bias and 92% at a few volts bias. Optimum p-layer thickness for high efficiency was found to be in the range $2-2.5 \mu m$. P-layer thickness less than $1.5 \mu m$ led to contacting problems during processing, and tended to yield unacceptably high reverse leakage currents, possibly as a result of the high strain under the sintered ring contacts. A typical device response as a function of wavelength is reproduced in Fig. 6 where the fall-off in response at shorter wavelengths arises from surface recombination effects, and the sharper decrease at long wavelengths reflects the absorption edge. Peak response at $1.15 \mu m$ was obtained by adjusting the alloy composition to 30% In.

The increase in the reverse leakage current as a function of ambient temperature at a given bias of a typical device is shown in Fig. 7. Although no extended life testing of the photodiodes has been carried out, devices were operated continuously at 100° C for several hours with no evident deterioration of the I-V characteristics or spectral response. Using a GaInAs $1.06 \,\mu$ m LED source the photoresponse of a typical device was measured as a function of temperature, as shown in Fig. 8. Although the $1.06 \,\mu$ m LED and photodiode were not response matched leading to a peak response at higher temperatures, the plot clearly illustrates that output variation within 5% may be maintained over a range of 100° C for response matched devices. The pulse response of the photodiodes was also measured using a pulsed

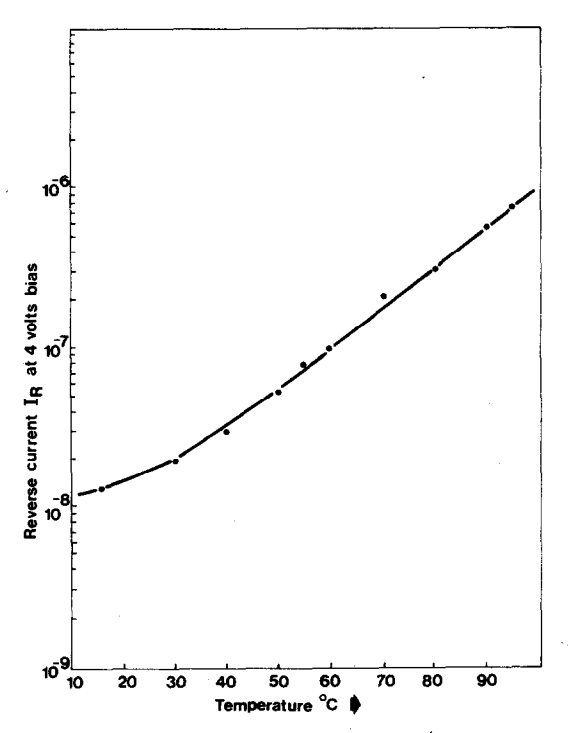


Fig. 7. Temperature dependence of dark current of GaInAs photodetector.

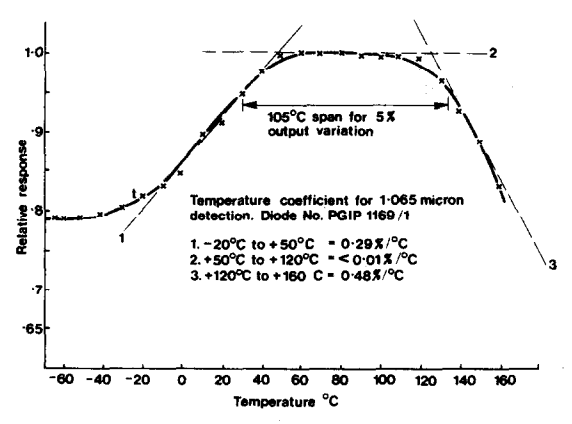


Fig. 8. Temperature dependence of photoresponse using 1.06 μ m LED source.

1.06 μ m LED source driven by a delay line pulse generator with a rise time of ~ 1 nSec. The detector risetime was found to be RC limited since the relatively large area (1 mm^2) and high doping density $(3 \times 10^{16} \text{-} \text{electrons/cm}^3)$ results in a high device capacitance, typically 200 pF at 5 volts reverse bias leading to risetimes of ~ 12 nSec into 50 Ω . However, by reduction of device area and doping level it is evident that risetimes of less than 1 nsec can be achieved.

6. CONCLUSION

The results obtained to date have demonstrated that 1.15 μ m photodetectors with quantum efficiencies well in excess of 80% may be fabricated using the Ga_{1-x}In_xAs ternary system. For high speed fibre optic applications low device capacitance is necessary, so that for a given area epitaxial layers with low background doping are required. It is expected that a number of modifications to the growth techniques which are currently being investigated will lead to lower background levels than hitherto obtainable. In addition, preliminary experiments have indicated that further reduction in the surface leakage currents may be achieved by a combination of proton bombardment isolation and oxide passivation techniques, in order to suppress edge breakdown effects. These improvements are likely to lead to efficient photodetectors optimised for applications out to 1.3 μ m and beyond.

Acknowledgements—The authors are grateful for financial support from the Procurement Executive, Ministry of Defence, DC VD, in carrying out this work, and to the Directors of Plessey Research (Caswell) Ltd for permission to publish the results. We are thankful to P. Augustus for the TEM photographs and many helpful discussions, and to F. Cotton and P. Staughton for help with the device processing.

REFERENCES

- S. E. Miller, E. A. J. Marcatili and T. Li, Proc. IEEE 61, 1703 (1973).
- 2. H. Kressel, J. Elec. Matr. 2, 1081 (1975).
- 3. C. J. Nuese, J. Elec. Matr. 6, 253 (1977).
- A. W. Mabbitt and C. D. Mobsby, Electron. Lett. 11, 157 (1975).

- 5. A. W. Mabbitt and R. C. Goodfellow, Electron. Lett. 11, 274 (1975).
- 6. R. C. Goodfellow and A. W. Mabbitt, Electron Lett. 12, 50 (1976).
- 7. C. S. Barratt, The Structure of Metals, p. 202. McGraw-Hill, New York (1943).
- 8. J. S. Ahearn Jr, C. Laird and C. A. B. Ball, Thin Solid Films 42, 117 (1977).
- 9. A. Hombert, Philips Res. Rep. 31, 216 (1976).
- 10. H. Ettenberg, C. J. Nuese, J. R. Appert, J. J. Gannon and
- R. E. Enstrom, J. Elec. Math. 4, 37 (1975).

 11. M. S. Abrahams and C. J. Buiocchi, J. Appl. Phys. 36, 2855 (1965).
- 12. D. J. Stirland, J. Mat. Sci. 9, 969 (1974).
- 13. H. Kressel, RCA Rev. June 1976, p. 175.